Comparative Study of the Diffusibility of a Nickel Alloy composed by Ni-Cr-Fe

Alima Carlos Averú[1], Luciano Volcanoglo Biehl[2],
Jorge Luiz Braz Medeiros[3]

[1,2,3]Universidade Federal de Rio Grande (FURG) – PPMec
Rio Grande/RS - Brasil

José De Souza[4]

[4]Fundação Liberato - Diretoria de Pesquisa e Produção
Industrial (DPPI)
Novo Hamburgo/RS - Brasil

Abstract—For this paper an Inconel Nickel alloy was produced by the Powder Metallurgy manufacturing process using Ni, Fe and Cr powder. From the new alloy two Samples - S1 and S2 - were produced with different percentages in the composition of the alloying elements. The Samples were compacted at 950 MPa according to ASTM B925-15 section 7 and sintered at 1200 °C in order to obtain an alloy and then to compare the best diffusibility between the alloying elements. The Samples were analyzed by Scanning Electron Microscopy (SEM) and with microprobe by Energy-dispersive X-ray Spectroscopy (EDS). In the results obtained Sample 1 showed a little diffusibility and Sample 2 had good diffusion.

Keywords— Powder metallurgy; Diffusibility; Nickel alloys.

I. INTRODUCTION

Powder metallurgy (PM) is a technique for the manufacture of metallic or ceramic compounds [1-2]. It consists of the transformation of the powder into a homogeneous and solid material [3]. It is manufactured with the application of a certain pressure and heating with temperatures below the melting point of the major constituent of the alloy [4]. In the processing for the manufacture of metal parts with powder metallurgy, it is necessary to perform basic steps: Powder extraction, characterization, powder mixing, compacting and sintering of the compacted being this final stage of the process [5].

Ni–Cr–Fe alloys are excellent because the maintenance of mechanical and corrosion properties even at elevated temperature [6]. Main advancements in powder metallurgy are related with the potential growth in their shape complexity and performance levels [7].

II. REWIEW OF SINTERING

A. *Sintering and densification*

In a study of the deposition of Chromium on steels with different compositions [8] the rearrangement of atoms in the substrate occurred in specific concentrations, around 13% to 1000 °C. In the Fe-Cr binary diagram, at temperatures between 825 and 1300 ºC the Chromium-Iron diffusion system presents a phase transition region due to the relative concentration of these elements [9].

At 1200 °C the diffusion of Chromium in the alpha phase (α) is 45% higher than in Iron gamma (γ). However, under a given isothermal heating, there is a discontinuity of diffusion of Chromium on the steel. The addition of a third element such as Nickel increases the solubility of the Chromium in CFC structures generating a rejection of this element in the crystalline structures CCC and getting accumulated in the phase (γ) [10].

The compacting procedure of the metallic powders has great influence on their final density. When necessary a higher percentage of densification and mechanical resistance is used the manipulation of the powders for the best contact between the particles. With the manipulation, the sintering can be more efficient by the practical and economic limitations of temperature and sintering time [11].

In sintering the compacted particles are bound by diffusion of atoms at high temperatures below the melting point of the base metal of the alloy. With the transport of atoms, under controlled conditions of time, temperature and atmosphere [12]. So that at the end of the process a solid, homogeneous material with desired properties and characteristics is obtained and as a consequence the decrease of the porosity of the part and the increase of the densification is obtained [4].

The sintering process can be understood by the mass transport mechanism (Fig. 1). The pores are as large accumulations of vacancies, facilitate the understanding of the sintering explained by its movement and consequently by the diffusion. Basically occur four atomic motion mechanisms in sintering: Surface diffusion, spread throughout the volume of grain boundary and by evaporation-condensation [12].
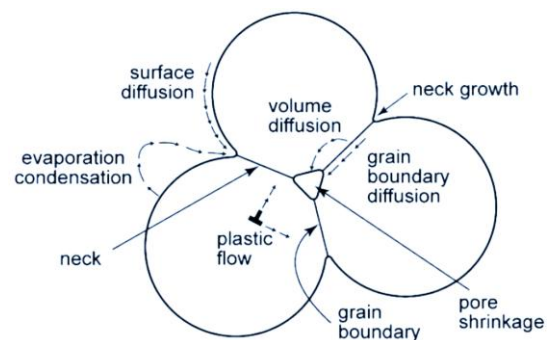

Fig. 1. Mechanisms of sintering [12].

It is essential during the sintering process to have the atmosphere controlled to minimize possible chemical reactions in the green compacted, removal of impurities that may exist in the form of oxide films [12]. The temperature and the residence time of the compacted in the furnace are important factors in the sintering. The longer the stay, the greater the bond strength and the particle size. This fact can be decisive, because the smaller its size the greater the degree of bond strength due to the existence of greater contact of the particulate, increasing the number of ways for the diffusion [4].

B. *Material diffusibility*

As the movements of the atoms through the crystalline lattice comes from the diffusion of the material in the solid state [13] diffusion can be classified into two main mechanisms, substitutional and interstitial diffusion [14-15].

The amount of atoms that move per time is due to the temperature and the concentration gradient. In this situation, the diffusion occurs to reduce the free energy of the system. The atoms of the more concentrated regions diffuse each other to diminish the region in both states reaching a balance. Fick's Laws have solutions for various systems and help predict fuzzy processes in alloying [16].

However, these Fick Laws mathematically assert that the concentration gradient itself induces a tendency of composition equilibrium in diffusion. However, its manifestation occurs in the initial stages of diffusion, where the gradient is larger, reducing the force as the process occurs [17].

The first Fick law (Eq. 1) is applied in the flow of atoms to fixed concentration gradients, in practical situations involving diffusion, diffusion flux and concentration gradient. For a specific point inside a solid vary over time a liquid depletion of the component that is in diffusion causes that the use of the first law is not more useful and is using the differential equation (Eq. 2) named as a Second Fick's law [15].

$$J = -D \frac{dC}{dx} \quad (1)$$

$$\frac{\partial C}{\partial t} = \frac{\partial}{\partial x}\left(D \frac{\partial C}{\partial x}\right) \quad (2)$$

III. MATERIALS AND METHODS

In the production of Nickel Inconel alloy for this work were used Nickel, Chromium and Iron elemental metallic powders. Nickel with a mean particle size of less than 27 μm and composed of 99.98% of Nickel. For Iron with a mean particle size of 150 μm as recommended by ASTM-B214 [18] with a composition of 99.99% of Iron. For Chromium with a mean particle size of less than 300 μm composed of 98.99% of Chromium.

The two Samples used in the comparative diffusibility analyzes have different amounts of the elements in the composition. As well as ASTM B214 [15] and other ASTM standards governing the manufacture of components for MP some authors show the need to characterize metal powders used in the alloying properties ensuring predictable and repeatable [19].

The final composition of the alloy for forming the sample (S1) was 72% Ni, 10% Fe and 18% Cr. The final composition of S2 was 73% Ni, 10% Fe and 17% Cr. Both compositions of the alloy to be formed were mixed separately into a mixed Y coupled with 10 grams for each sample of the alloy to be formed. They were compacted all into a cold isostatically rigid matrix at 950 MPa.

After compacting powders according to Standard [20-21] the compacted (pressed) to green (Fig. 2 - A) were sintered at 1200 °C in a 99% pure Argon controlled atmosphere furnace for 6 hours being removed from the furnace still at the

sintering temperature of 1200 °C and cooled to air - room temperature (Fig. 2 - B).
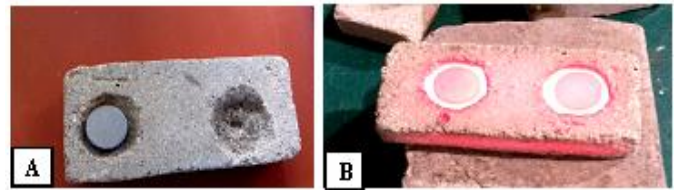

Fig. 2. (A) Compressed Sample to be sintered. (B) Sintered Sample cooling.

IV. RESULTS

A. *Characterization of metallic powders*

For the picture obtained on SEM (Fig. 3) there is an indication of particle size distribution of the metallic Nickel powder with a cubic morphology with small acicular shapes with average particle size less than 27 μm.
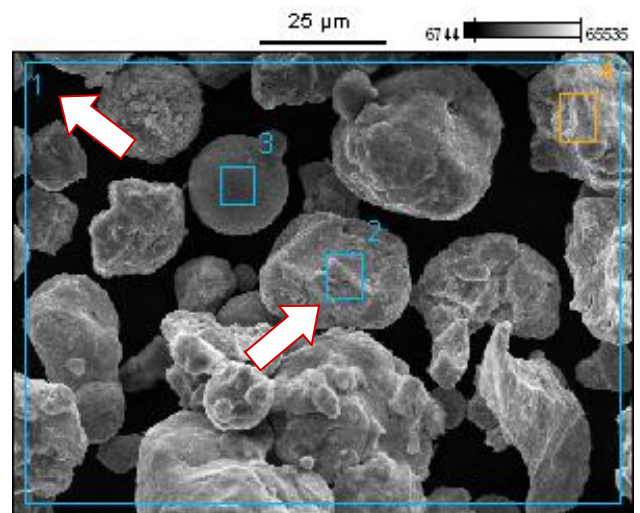

Fig. 3. Characterization of Nickel powder with SEM.

With the use of EDS microprobe the characteristic "peak" of Nickel can be verified (Fig 4).
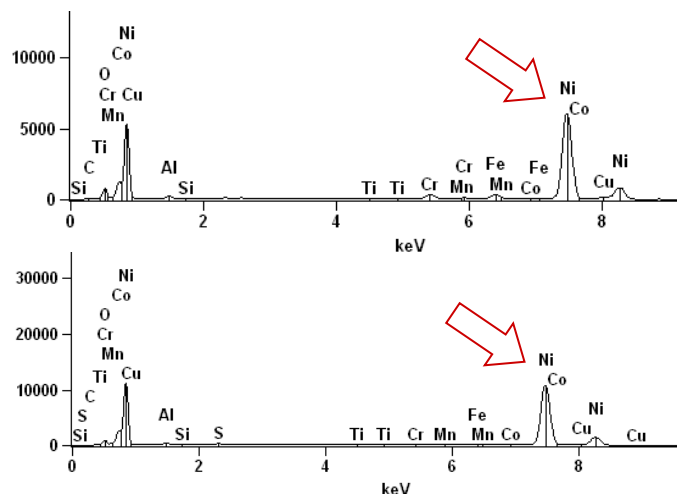

Fig. 4. EDS microprobe identifying Nickel characteristics. Points 1 and 2.

For the Iron powder the existence of particles between 5 and 150 µm (Fig. 5) with spherical morphology was verified. EDS microprobe showed the "peak" of the Iron (Fig. 6).
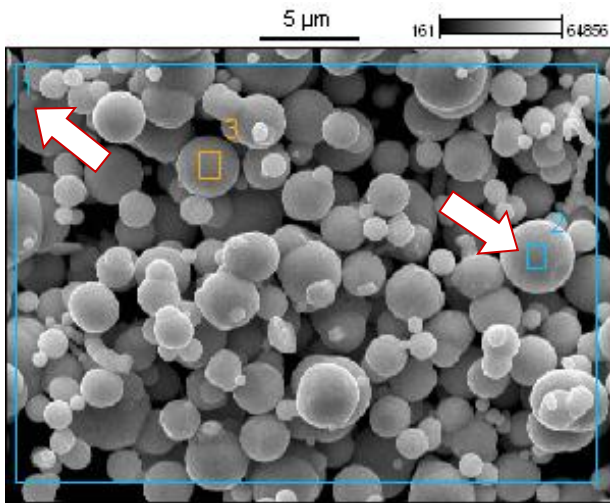

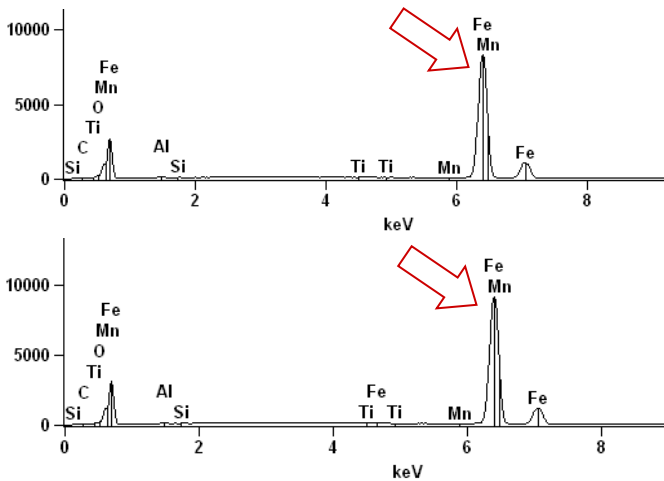Fig. 5.   Characterization of the iron powder by SEM and EDS.

Fig. 6.   EDS microprobe identifying Iron peak. Points 1 and 2.

Chromium powder is morphologically angular with acicular shapes and with an average particle size of less than 300 µm (Fig. 7).
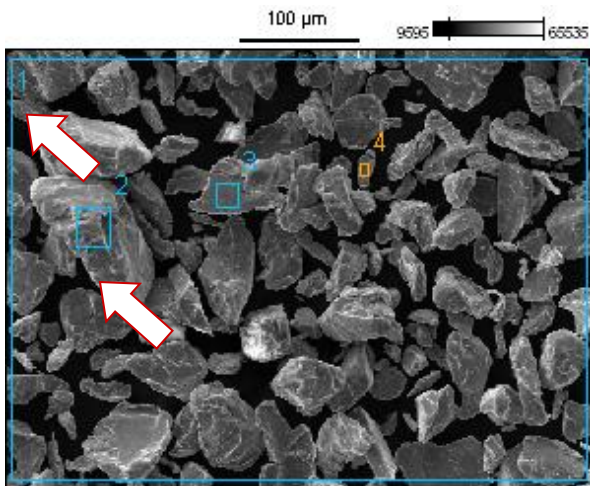

Fig. 7.   Characterization of Chromium powder by SEM.

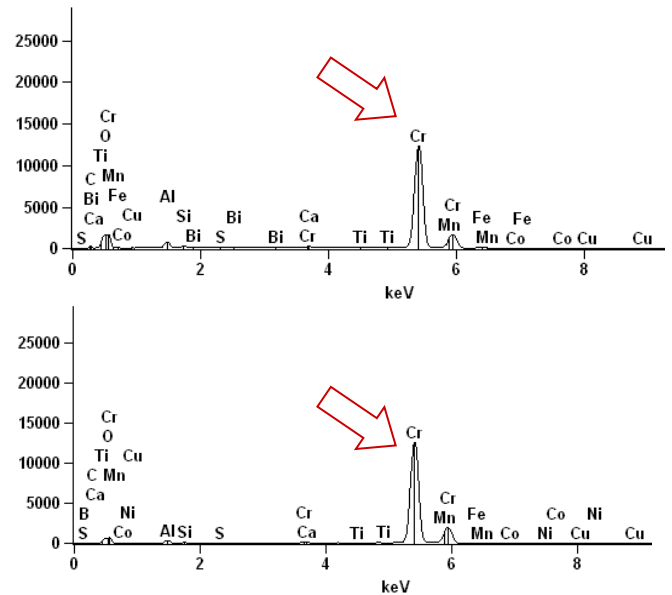The typical "peak" of Chromium (Fig. 8) is identified with EDS microprobe.

Fig. 8. EDS microprobe identifying Chromium peak. Points 1 and 2.

Even with the granulometric differences between the powders, the images show similarities between Chromium and Iron powder. These two have a larger particle size than the Nickel powder.

As the Chromium dissolves for the most part in the interstitial form in the Iron this hinders the output of the carbon contained therein. The similarity that the SEM images demonstrate in the Chromium and Iron powder grains is favorable for good diffusivity between them in the sintering.

The morphology as the shape of the grains and the degree of homogeneity of the particles has an important effect on the characteristics of the compacted ones and for the final process. Irregular forms are more susceptible to deformation, which generates greater contact between particles and higher density [22].

Each of the three powders used in this research were individually analyzed by EDS proportional to the SEM. The chemical elements present in each metal powder were verified, whether or not there was contamination by other constituents, and the percentage of the content of each element.

B. SEM analysis and EDS mapping of sintered Samples

Results of the SEM analyzes sintered and the mapping of the region via EDS showed an image of the regions analyzed in S1 and S2. It was obtained by the variation of backscattered electrons evidenced by the mapping of the filtered elements contained in the same region (Fig. 9 - 10).

By adding alloying elements in a steel it is essential to place elements which are dissolved within the interstitial Iron or so as to replace it. The Chromium element dissolves in the interstitium. This prevents the exit of the carbon causing a good diffusibility between the elements, achieving in part to have slow cooling rates of the alloy.

Published by :

http://www.ijert.org

International Journal of Engineering Research & Technology (IJERT)
ISSN: 2278-0181
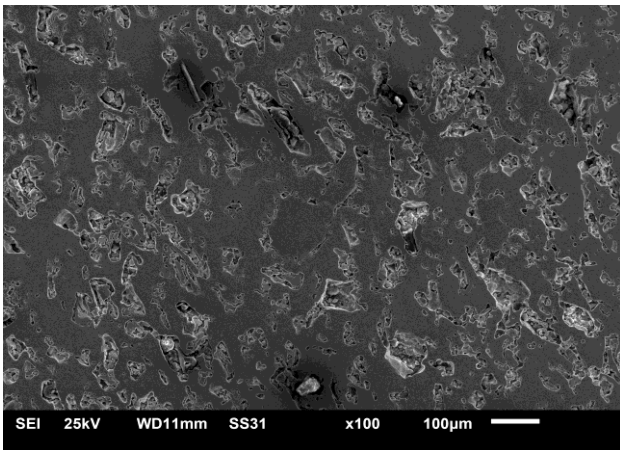**Vol. 5 Issue 12, December-2016**
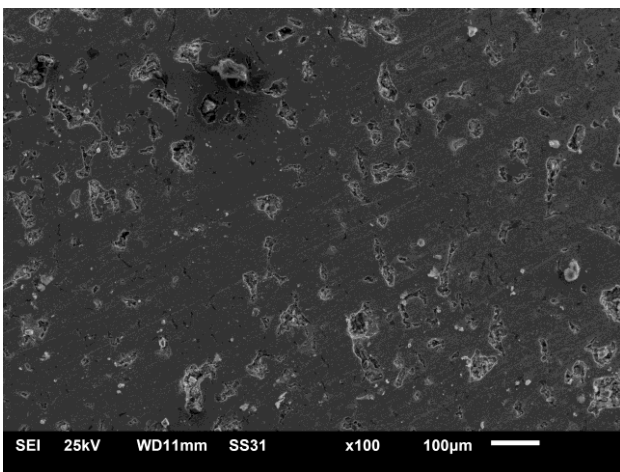
Fig. 9.   Mapping of Sample 1.

Fig. 10. Mapping of Sample 2.

In the MEV images (Fig. 9-10) the Samples S1 and S2 exhibit irregular pores confirming the existence of macropores and interconnected micropores that favor the diffusion between the alloying elements. There was a greater irregularity in sample S1 than in S2. In the dark spots, we see less porosity in S1 with closer acicular angular pores. This shape seen in the Chromium powder morphology evidences the weak diffusibility of Chromium with other alloying elements. The qualitative evaluation of the elements contained in the Samples S1 and S2 (Fig. 11-12) made by the EDS technique with its mapping of the constituent elements in a filtered form elucidating the elemental composition for each of the Samples.
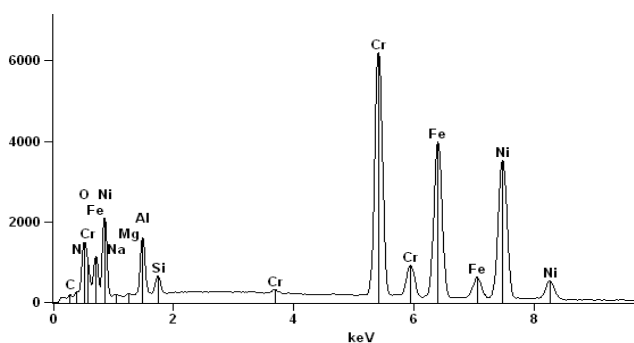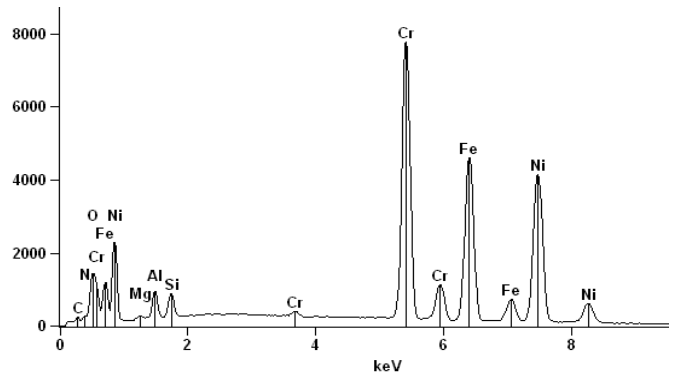

Fig. 11. EDS Sample 1 with irregular pores.

Fig. 12. EDS Sample 2 with the elements.

In the S1 spectrometry (Fig. 11) the SEM showed that there was a low diffusibility of atoms that have more porosity in the dark spots. This results in no increase in densification as reported research cited [1-8]. The diffusion of the elements contained in the S1 in a filtered form was verified (Fig. 11), where the chromium was the element that revealed itself with a higher content and did not diffuse perfectly with other elements of the alloy, causing it to be revealed with greater Graphic peak.

In the mapping of S1 (Fig. 13) the weak diffusibility of the alloying elements, Chromium and Iron in most of the analyzed region, is observed. The regions of lower intensity of the map of Chromium in green and of lower intensity in the map of the Iron shown consequently that there was a bad distribution, evidencing the weak diffusibility between these elements. In the region where there is more intensity in the map of the Iron in red, medium intensity in the map of the Chromium and less intensity in the map of the Nickel in blue.
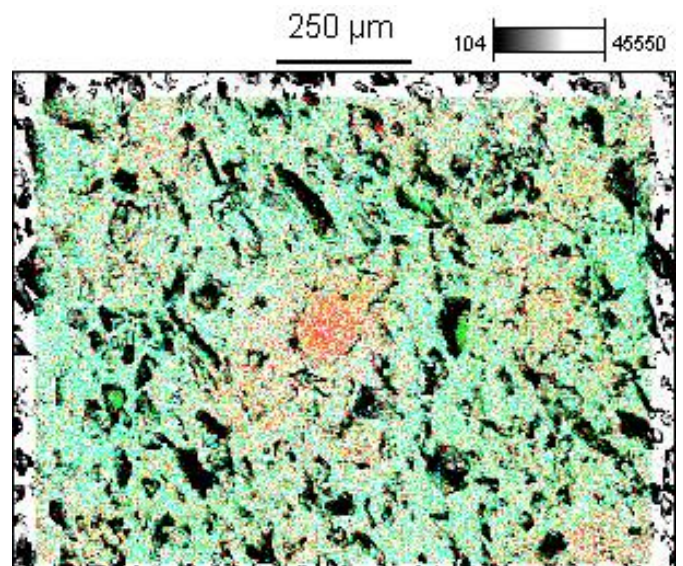

Fig. 13. Diffusibility of the elements in the Sample 1.

The results of the S2 spectrometry of the alloy (Fig. 14-15), different from S1, showed better diffusion with smaller pores, even though the graph also shows Chromium as having a high alloy content. S2 was shown to have better diffusivity with other alloying elements in S2.
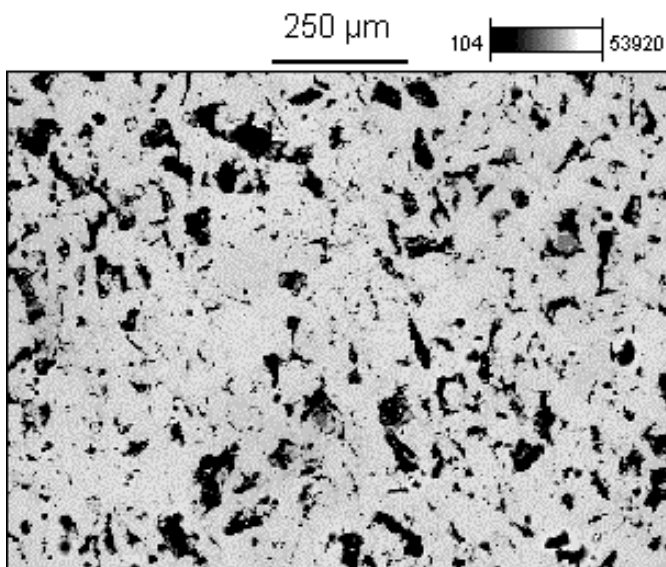
Fig. 14.   EDS Sample 2 with less pores than Sample 1.

The mapping of the Nickel Inconel alloy formed in S2 (Fig. 15) analyzed by the EDS technique shows good distribution and is much more prone to differences in concentration. It also shows good diffusion by the smaller amount of the Chromium contained therein from the mixture of the composition at the beginning of the process of the formation of the alloy.
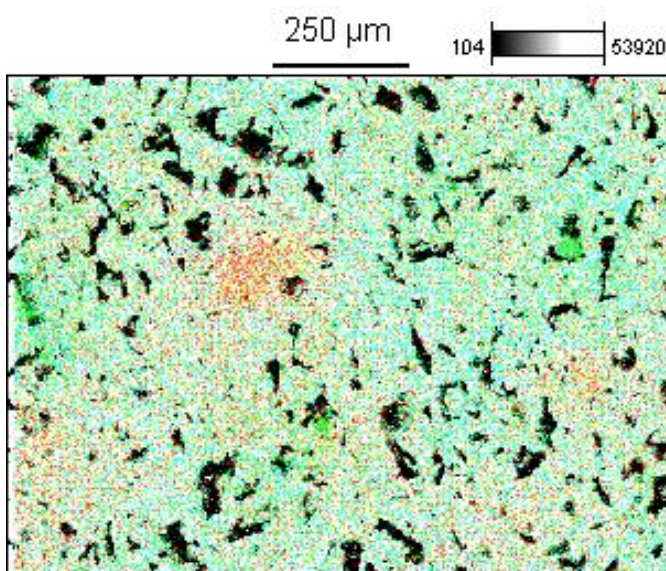

Fig. 15. Diffusibility of the elements in the Sample 2.

V.   CONCLUSIONS

From the presented research, it is verified the difficulty in obtaining a solid, homogeneous material by the sintering of elemental metallic powders. Here we see the difficult occurrence of diffusibility between alloying elements, an example that can occur in Inconel alloys. The result of the S2 sample proved this situation in which there was better diffusibility in relation to the S1 sample.

It is suggested that for future research, that they use a lower content of Chromium and Iron, increasing Nickel, because with more Chromium it is difficult to obtain good diffusion that results in a higher degree of porosity as occurred in sample S1. It is also suggested that a variation of the sintering time be applied and another inert gas (Nitrogen or Helium) should be used to control the atmosphere of the furnace during the sintering of the alloy. Probably under these conditions, a better diffusibility will be obtained in relation to what was obtained in S2 of this research.

Although S2 proved to be better than S1 diffusely both Samples analyzed did not show total dissolution between the elements. The region analyzed by the EDS technique showed a small region with more Iron (Fig. 14 - 15) than other elements, due to the low densification, although the overall mixture had a different ratio.

ACKNOWLEDGMENT

REFERENCES

[1]   J. de Souza; C. A. Oliveira-Motta; T. G. Machado; A. Giacomin and H. M. A. Arabi. Analysis of Metallic Waste from Laser Cutting for Utilization in Parts Manufactured by Conventional Powder Metallurgy. International Journal of Research in Engineering and Science (IJRES). Vol.4 Issue 11-November, 2016. p.01-05.

[2]   J. de Souza; A. P. Borba; C. A. Oliveira-Motta; V. Martins and L. Schaeffer. Projeto de fabricação de face cilíndrica estacionária para biorreatores anaeróbios. Revista Liberato, Novo Hamburgo, v. 13, n. 19, p. 01-76, jan./jun. 2012.

[3]   J. de Souza; C. A. Oliveira-Motta; and L. Schaeffer. Utilización de Ceniza Volante Aleada al Material Compuesto Hierro-Cobre-Grafito mediante un Proceso de Pulvimetalurgia. Información Tecnológica. Vol. 25(5), 21-26 (2014)

[4]   N. de A. Braga; N. G. Ferreira and C. A. A. Cairo. Obtenção de titânio metálico com porosidade controlada por metalurgia do pó. Química Nova, Vol. 30, No. 2, 450-457, 2007.

[5]   M. C. Rezende; L. S. Araújo; S. B. Gabriel; J. Dille and L .H. de Almeida. Oxidation assisted intergranular cracking under loading at dynamic strain aging temperatures in Inconel 718 superalloy. Alloys and Compounds, Volume 643, Supplement 1, 15 September 2015, pg S256–S259, 2014.

[6]   H. Li; S. Xia; W. Liu; T. Liu and B. Zhou. Atomic scale study of grain boundary segregation before carbide nucleation in Ni–Cr–Fe Alloys. Journal of Nuclear Materials 439) 57–64, 2013.

[7]   W. H. El-Garaihy; A. Nassef and M. El-Hadek. Comparative study of different alloys during thermal debind-ing of powder injection molded parts. International Journal of Engineering & Technology, 5 (4) 110-114, 2016.

[8]   R. Drewett. Diffusion coatings for the protection of iron and steel, Anti- Corrosion Methods and Materials, Vol. 16, N. 6, pp. 10 - 14, 1969.

[9]   R. Jha; C. W. Haworth and, B. B. Argent. The Formation of Diffusion Coatings on some Low-Alloy Steels and their High Temperature Oxidation Behaviour: Part 1 Diffusion Coatings. Calphad, Vol. 25, No. 4, p. 651-665, 2001.

[10] E. Lassner and W. D. Schubert. Tungsten - Properties, Chemistry, Technology of the Element, Alloys, and Chemical Compounds – Vienna University of Technology, Vienna, Austria - p. 321 - 362, 2010.

[11] R. M. German. Coarsening in Sintering: Grain Shape Distribution, Grain Size Distribution, and Grain Growth Kinetics in Solid-Pore Systems. Critical Reviews in Solid State and Material Sciences 35(4):263-305, November 2010.

[12] M. P. Groover. Fundamentals of Modern Manufacturing: Materials, Processes, and Systems. 4° ed. John Wiley & Sons. 2010.

[13] D. R. Askeland; P. P. Fulay and D. K. Bhattacharya. Essentials of Materials Science and Engineering, SI Edition, Second Edition, Cengage Learning. 2010.

[14] S. J. L. Kang. Sintering, Densification, Grain Growth and Microstructure. Elsevier. 2005.

[15] W. D. Jr. Callister, Ciência e Engenharia de Materiais: Uma Introdução, Rio de Janeiro, Ed. LTC. 2002.

[16] ASM - American Society of Metals. Elements of Metallurgy and Engineering Alloy. ASM International. 2004.

[17] M. A. Ashby. First Report On Sintering Diagrams, Acta Metallurgica, Vol 22. 1974.

[18] ASTM - American Society for Testing and Materials. ASTM B214 Standard Test Method for Sieve Analysis of Metal Powders, West Conshohocken, USA, 2015.

[19] E. J. Slotwinski; J. A. Garboczi; P. E. Stutzman; C. Ferraris; S. S. Fwatson and M. A. Peltz. Characterization of Metal Powders Used for Additive Manufacturing, Journal of Research of the National Institute of Standards and Technology, Vol. 119. 2014.

[20] ASTM - American Society for Testing and Materials., 2008 ASTM B925 Standard Practices for Production and reparation of Powder Metallurgy (PM) Test Specimens, West Conshohocken, USA.

[21] ASTM International. 2015. ASTM B962 Standard Test Methods for Density of Compacted or Sintered Powder Metallurgy (PM) Products Using Archimedes' Principle, West Conshohocken, USA.

[22] C. L. Martin; D. Bouvard and S. Shima. Study of particle rearrangement during powder compaction by the Discrete Element Method. Journal of the Mechanics and Physics of Solids Vol. 51, 2003. p. 667 - 693.